

## CFD, A DESIGN TOOL FOR A NEW HOT METAL DESULFURIZATION TECHNOLOGY

Stefan PIRKER<sup>1</sup>, Philipp GITTLER<sup>1</sup>, Hermann PIRKER<sup>2</sup> and Joachim LEHNER<sup>2</sup>

<sup>1</sup> Johannes Kepler University, 4040 Linz, AUSTRIA, e-mail: pirker@mechatronik.uni-linz.ac.at

<sup>2</sup> VOEST ALPINE Industrieanlagenbau GmbH, Postfach 3, 4031 Linz, AUSTRIA

### ABSTRACT

A big vessel contains hot metal covered by a thick synthetic slag layer. During nitrogen stirring sulfur transits to the slag. Sulfur ions in the slag have to be removed by oxidation (O<sub>2</sub> lance) to restore slag desulfurization capability.

The macroscopic metallurgical reactions occurring during hot metal desulfurization and slag regeneration are studied by kinetic laws for permanent and transient phase contact. Mechanical metal-slag interactions are calculated by shear stress considerations for stratified flows. The position of the phase interface and the slag surface is obtained by an adaptive grid algorithm. Flow initiation by rising gas bubbles is simulated by means of an algebraic drift flux model.

As a result of these simulations the fully three-dimensional flow- and temperature fields in the slag and metal phase are obtained. Furthermore the variation of the time-dependent concentration fields of the main reactants can be observed.

### NOMENCLATURE

$A$	area
$g$	gravitational acceleration
$h$	bath height
$\Delta H$	molar reaction enthalpy
$J_0$	initial nozzle momentum
$K_S$	equilibrium constant for slag regeneration
$L_S$	equilibrium constant for sulfur removal
$M_S$	molar weight of sulfur
$Q$	heat content
$p$	static pressure of fluids, partial pressure of gases
$t$	time
$T$	temperature
$u$	velocity
$V$	volume
$\Delta z$	deformation of free surfaces
$\alpha$	gas volume fraction, heat transfer coefficient
$\varepsilon$	emission coefficient
$\kappa$	mass transfer coefficient
$\mu$	viscosity
$\rho$	mixture density
$\sigma$	Stefan-Boltzmann constant
$\tau$	shear forces

subscripts:

$b$	bubble
$c$	cell
$drift$	drift (-velocity)
$e$	environment
$f-str$	free-stream
$g$	gas
$hm$	hot metal
$inter$	metal $\leftrightarrow$ slag interface
$react$	reaction
$sl$	slag
$surf$	bath surface
$tr$	terminal rising (-velocity)
$wall$	wall and bottom lining of the vessel
$lam$	laminar
$turb$	turbulent

chemical nomenclature:

[ ]	mass fraction of species dissolved in hot metal
( )	mass fraction of species dissolved in slag
{ }	mass fraction of gaseous species

### INTRODUCTION

This new desulfurization technology, which is investigated by means of CFD-simulations, can be divided into two process steps. First the dissolved sulfur transfers from the hot metal into the synthetic slag layer during the hot metal desulfurization. This process is considered in the next two chapters. Second the synthetic slag has to be regenerated by oxygen injection after reaching its sulfur capacity. This second step can be studied independently from the first one. After the slag regeneration new hot metal can be desulfurized and the process starts from its beginning. During the development of the simulation models care is taken to create results that are comparable with ongoing high temperature experiments.

### SIMULATION OF THE DESULFURIZATION PROCESS - MODELLING

Hot metal and slag are both considered as Newtonian fluids. As a consequence the well known Reynolds averaged Navier-Stokes equations have to be fulfilled in both phases. The turbulent characteristics of the flow pattern are modelled by the standard k- $\varepsilon$  model (Launder and Spalding, 1972). Species transport, i.e. sulfur transport in the hot metal or sulfur ions transport in the slag phase, is calculated by means of a scalar transport equation considering convective and diffusive transport mechanism (Patanker, 1980). Turbulent diffusion is calculated by applying a constant Schmidt number

(Prandtl et al, 1993). For the simulation of the temperature field an additional energy transport equation is introduced accounting for heat transport based on convection and conduction. In principle calculations are performed in hot metal and slag independently. Reciprocal influence, i.e. mechanical and chemical, is assumed to happen only at the metal-slag interface.

### Shear Stress Considerations at the Metal-Slag Interface

If the bath agitation is not too strong and emulsification does not occur, the two fluids, hot metal and slag, represent stratified flow conditions. To explain the modelling of the reciprocal mechanical influence at the interface a Couette flow is considered.

A hot metal phase and an upper slag layer is situated between two parallel horizontal plates. The upper plate moves with constant velocity  $u_c$  to the right. Because of the no slip condition the uppermost slag layer has to move with the same velocity. On the phase-interface in the middle between the plates shear forces act from both the hot metal as well as from the slag. In the equilibrium state they have to nullify each other:

$$\tau_{sl \rightarrow inter} = \tau_{hm \rightarrow inter} \quad (1)$$

In the computer code this principle is implemented by a moving interface wall. The velocity of that fictitious wall has to be in between the velocities in the neighboring hot metal and slag cells. The exact value of the wall velocity at a given position can be calculated by comparing the shearforces acting from the hot metal flow with those acting from the slag layer.

Figure 1 shows the calculated results in the case of turbulent Couette flow. In this simulation slag viscosity is supposed to be ten times higher than hot metal viscosity.

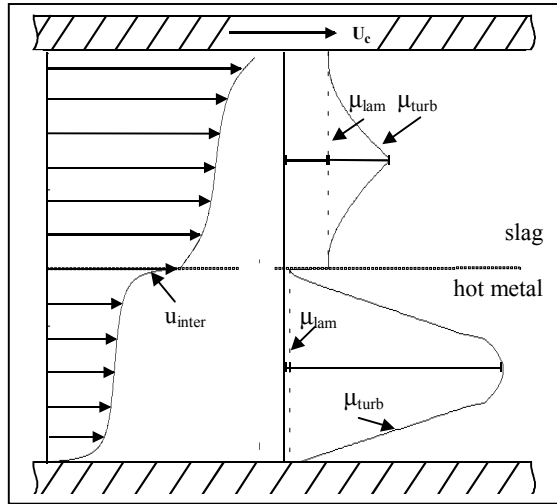


**Figure 1:** Turbulent Couette Flow.

The computed velocity profile is displayed on the left side. In the laminar sublayers of the hot metal phase higher velocity gradients exist due to its lower laminar viscosity. On the right side the effective viscosity formed by the sum of the laminar and turbulent viscosity is

shown. Although hot metal phase laminar viscosity is lower than that of the slag, its effective viscosity is higher than the effective slag viscosity. This surprising result can be explained by the different thickness of the boundary layers. In the slag phase turbulent fluctuations are suppressed by the thicker boundary layers. As a consequence of this effect the velocity gradients in the middle of the hot metal layer are smaller than in the middle of the slag.

### Position of Phase Interface and Bath Surface

A hydrostatic deformation of the free surfaces can be deduced from the differences in the pressure distribution at the phase interface and the bath surface:

$$\begin{aligned} \Delta z_{hm} (\rho_{hm} - \rho_{sl}) g &= p - (h_{sl} \rho_{sl} g + p_e), \\ \Delta z_{sl} \rho_{sl} g &= p - p_e. \end{aligned} \quad (2)$$

After deformation both fluid volumes have to be rescaled in vertical direction in order to fulfil the mass balances in each phase. The deformation of the free surfaces influences the flow field in the liquid phases and as a consequence the sulfur transport to and from the surface. Therefore this calculation is included into the simulation although it is not of major importance for the desulfurization rate at first glance.

### Bath Agitation by Nitrogen Injection

In order to stir the bath, nitrogen is injected through a porous plug at the bottom of the vessel. The uprising gas bubbles induce a flow in the continuous phases of hot metal and slag. The effect of the gas bubbles is accounted for by an algebraic slip model (Manninen et al, 1996).

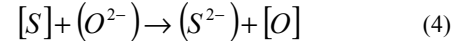
This mixture model is supplemented by a more general calculation of the drift velocity between the gas bubbles and the continuous phases. In this simulation the drift velocity is set to (Prandtl et al, 1993).

$$u_{drift} = (1 - \alpha_g)^{1.39} u_{tr}. \quad (3)$$

The gas bubbles are assumed to pass the metal-slag interface without rest and to leave the slag phase at the bath surface immediately.

### Sulfur Transfer

At the phase interface dissolved sulfur migrates from the hot metal to the slag phase:



The rate of sulfur loss in a cell adjoining the metal-slag interphase is assumed to be proportional to the difference between a free stream sulfur concentration and the equilibrium sulfur concentration at the phase interface:

$$\begin{aligned} \frac{d[S]_c}{dt} \cdot M_{c, hm} &= \\ \kappa_{hm \leftrightarrow sl} \cdot A_c \cdot \left( [S]_{f-str} - \frac{(S^{2-})_{inter}}{L_s} \right) \end{aligned} \quad (5)$$

The same sulfur mass flow has to be added in the very slag side cell:

$$\frac{d[S]_c}{dt} \cdot M_{c,hm} = -\frac{d(S^{2-})_c}{dt} \cdot M_{c,sl} \quad (6)$$

The mass transfer coefficient  $\kappa$  is influenced by velocity and turbulence fields and can be predicted by empirical correlations (Deo and Boom, 1993). However, in this simulation it is kept constant. It is only varied in two simulations from 0.1 to 1 kg/m<sup>2</sup>s to show the principal dependencies on this parameter.

### Temperature Field

At the outer walls and the bottom of the vessel a heat flux condition is set:

$$\dot{Q}_{wall} = \alpha_{wall} \cdot A \cdot (T - T_e) \quad (7)$$

At the bath surface heat is lost due to convection and radiation:

$$\frac{\dot{Q}_{surf}}{A} = \alpha_{surf} \cdot (T - T_e) + \varepsilon \cdot \sigma \cdot (T^4 - T_e^4) \quad (8)$$

The heat transfer coefficients as well as the emissivity coefficient can be found in literature (Oeters, 1989). The sulfur transfer is linked to the temperature field by the reaction enthalpy

$$\dot{Q}_{react} = \frac{d[S] M_c}{dt M_s} \Delta H_{react} \quad (9)$$

while the cooling effect of the incoming nitrogen is neglected in these simulations.

## SIMULATION OF THE DESULFURIZATION PROCESS – RESULTS

Numerical simulations are performed by a modified and enhanced FLUENT code on a SGI Indigo workstation.

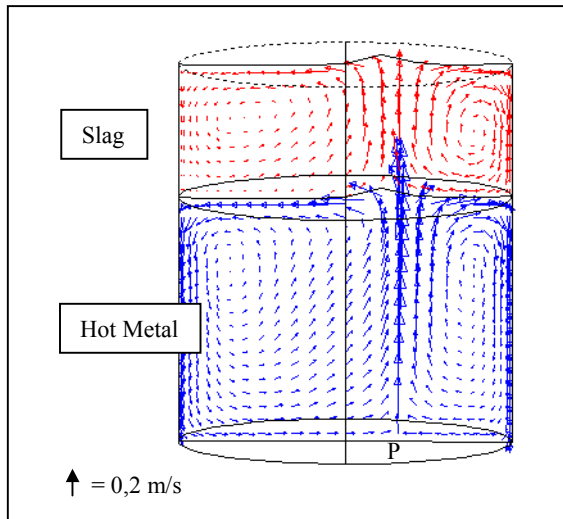


**Figure 2:** Velocity Field in Slag and Hot Metal (P=Porous Plug).

As hot temperature experiments are not available at the moment the feasibility of the simulation technique is proven of parametric studies.

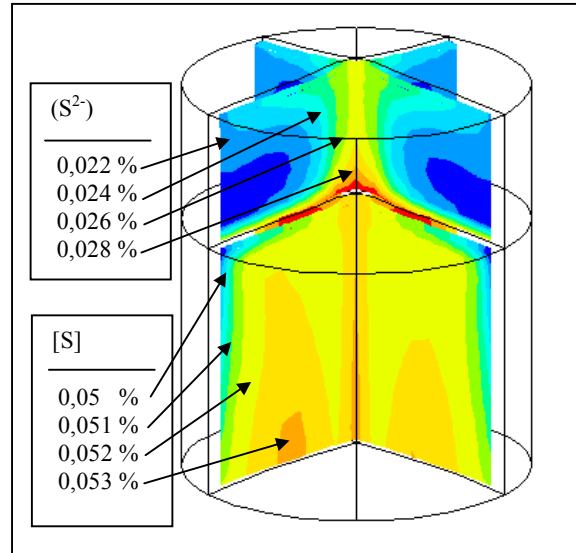


**Figure 3:** Sulfur Content in Hot Metal and Slag after 1 min. of Desulfurization ( $[S]_0 = 0,06 \%$ ).

Figure 2 shows the velocity field in both phases during eccentric nitrogen injection. In the region of the uprising bubble plume the deformation of the free surfaces can be seen.

In Figure 3 the sulfur concentration in both phases one minute after the beginning of desulfurization is displayed.

In Figure 4 the transient sulfur content in both phases is given. Several parameter studies are performed to show the functionality of the simulation model. The variation of both the thermodynamic equilibrium  $L_s$  as well as the sulfur transfer coefficient  $\kappa$  influence the desulfurization curves in a reasonable way.

A higher gas throughput causes higher fluid velocities and therefore increases the desulfurization rate due to improved sulfur transport to and from the phase interface. This clearly shows the purpose of CFD in the prediction of mass transport controlled interfacial reactions. The flow pattern in the liquid phases influences the reaction rate distribution at the phase interface directly. With the help of CFD it can be shown that the desulfurization rate varies with the gas flow rate as well as with the position of the porous plug on the bottom of the vessel or the vessel geometrie. These results cannot be obtained by conventional mixed reactor models.

## SIMULATION OF THE SLAG REGENERATION PROCESS – MODELLING

During the slag regeneration process oxygen is blown through a submerged lance into the slag phase, which is enriched with sulfur-ions by that time. Once injected the oxygen reacts with the sulfur to gaseous sulfur dioxide which forms the offgas of the process. While developing the simulation tools special attention was given to the comparability of simulation results with first high temperature experiments.

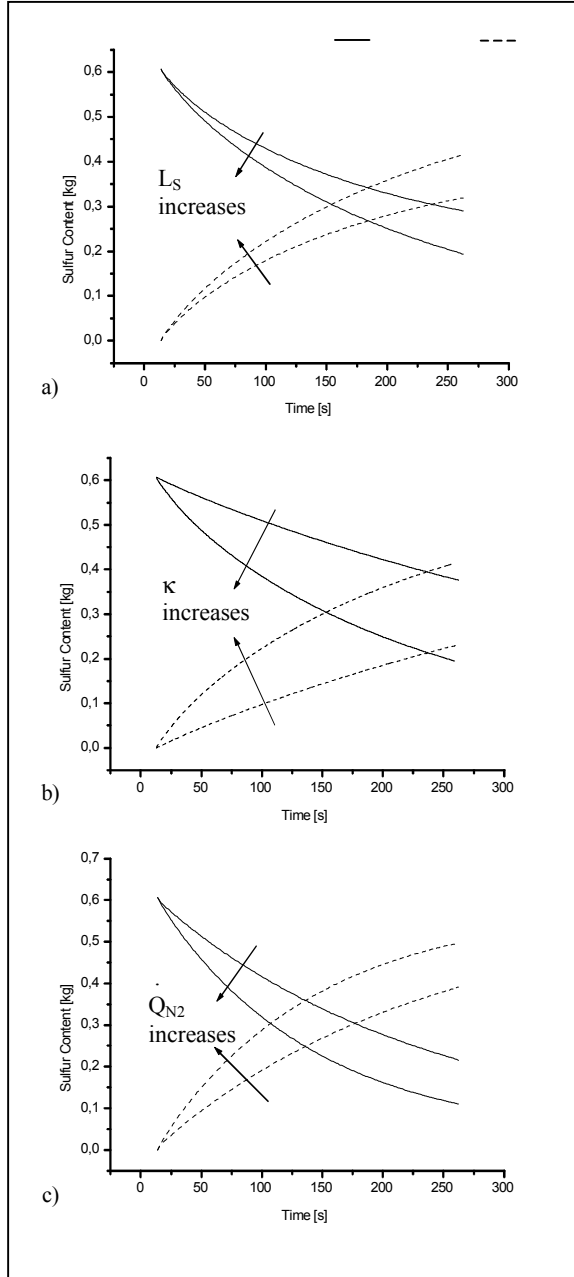


**Figure 4:** Parametric studies of the desulfurization process: Sulfur content in hot metal (—) and slag (---).

### Bath Agitation by Oxygen Injection

Basically the same mixture approach as described in the previous chapter is applied. Nevertheless, two new aspects have to be considered in this configuration.

First, the initial momentum of the incoming gas is no longer negligible and has to be added to the Navier-Stokes equations as a source term:

$$I_0 = \dot{V}_{O_2} \cdot \rho_{O_2} \cdot u_0 \quad (10)$$

Second, the production of  $\{SO_2\}$  and  $(CaO)$  has to be accounted for. Due to this reaction the total volume of

the gas bubbles in the vessel is less than in the case of inert gas purging with identical incoming gas flow rate.

### Bath Swelling due to Gas Injection

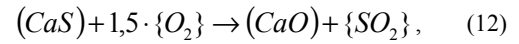
In this simulation approach the upper bound of the calculation domain is considered to coincide with the bath surface. At the beginning of gas injection the surface will rise due to the additional gas volume inside the slag phase. Therefore the computational grid has to be adapted each time step in order to fulfil the global mass balances:

$$\frac{d}{dt} \left( \int_V \rho \cdot dV \right) = \dot{V}_{O_2} \cdot \rho_{O_2} - \dot{V}_{Offgas} \cdot \rho_{Offgas} \quad (11)$$

The influence of grid movement is considered in all field equations (Fluent, 1996). Although the calculation of the bath height is not believed to be of major importance for the prediction of desulfurization it is included into this simulation to get just another variable which can be compared with experiments.

### Chemical Reaction

The main reaction occurring is given by (Glovaskii, 1982)



with the thermodynamical equilibrium constant

$$K_{reg} = \frac{(CaO) \cdot p_{SO_2}}{(CaS) \cdot p_{O_2}^{1,5}}. \quad (13)$$

The reaction takes place at the interface between the uprising gas bubbles and the liquid slag. In this case the reaction area in a computational cell is given by

$$A_{react} = 3 \cdot V_c \cdot \frac{(\alpha_{O_2} + \alpha_{SO_2})}{r_b}. \quad (14)$$

It directly depends on the mean radius of the gas bubbles. Obviously smaller bubbles are chemically more efficient than big ones.

The rate of sulfur loss in a cell is given by a mass action law and follows to:

$$\frac{d(S^{2-})_c}{dt} M_c = \kappa_{sl \leftrightarrow b} \cdot A_{react} \cdot \left( (CaS) \cdot p_{O_2}^{1,5} - \frac{(CaO) \cdot p_{SO_2}}{K_{reg}} \right) \quad (15)$$

The mass transfer coefficient  $\kappa$  is set to  $0.1 \text{ kg/m}^2\text{s}$  in this simulation. In futur simulations mass transfer correlations (Ray, 1993) should be used to account for the influence of velocity and turbulence fields on the mass transfer coefficient.

### Temperature Field

Basically the modelling is the same as in the case of the desulfurization process.

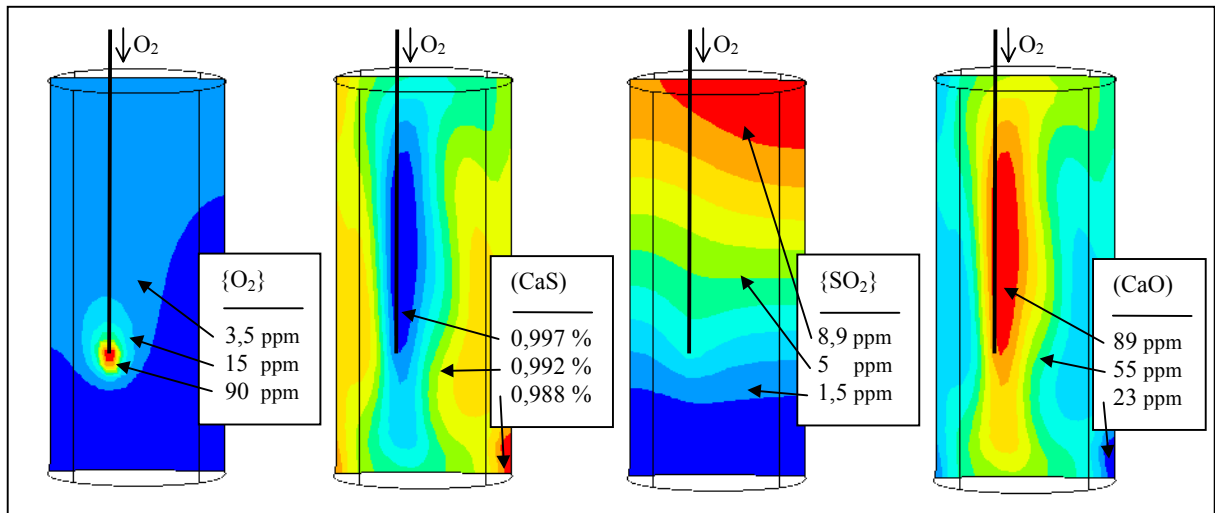


**Figure 5:** Spatial distribution of the main reactants during slag regeneration shortly after the beginning of the blow, Initial conditions: 1 % (CaS) and all others 0 %.

### SIMULATION OF THE SLAG REGENERATION PROCESS – RESULTS

Parametric studies demonstrate the expected tendencies in the reaction rate. The following parameter variations result in an improved reaction rate:

- Reduction of mean bubble diameter
- Reduction of atmospheric pressure (vacuum process)
- Reduction of partial gas pressures by additional inert gas purging
- Increased O<sub>2</sub> flow rate

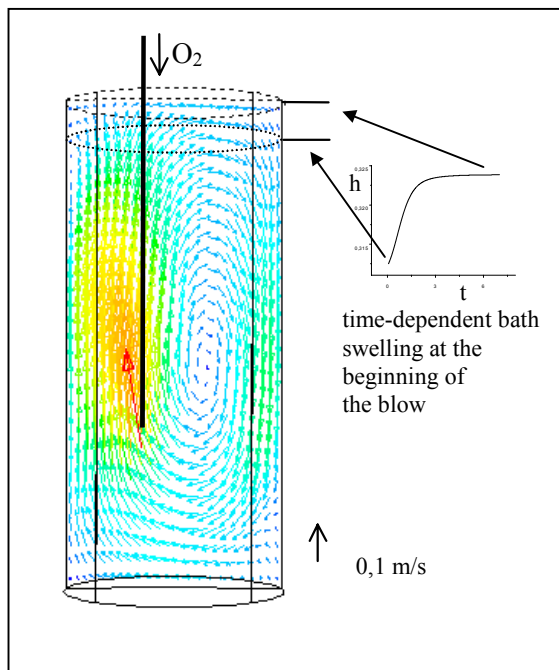


**Figure 6:** Velocity field in the slag vessel during slag regeneration including calculation of initial bath swelling

While simulating metallurgical processes the question arises how calculation results can be compared with real measurements. In the planned hot temperature experiments the following variables seem to be measurable:

- slag surface velocity (by video methods)
- surface temperature (by infrared thermometer)
- bath height (by video methods)
- offgas composition (by in situ gas analysis)
- sulfur content (by conventional probe)

Figure 6 shows the velocity in the slag phase one minute after the beginning of oxygen injection. As a further result the transient rising of the bath surface is calculated. Both results can be compared with hot temperature measurements.

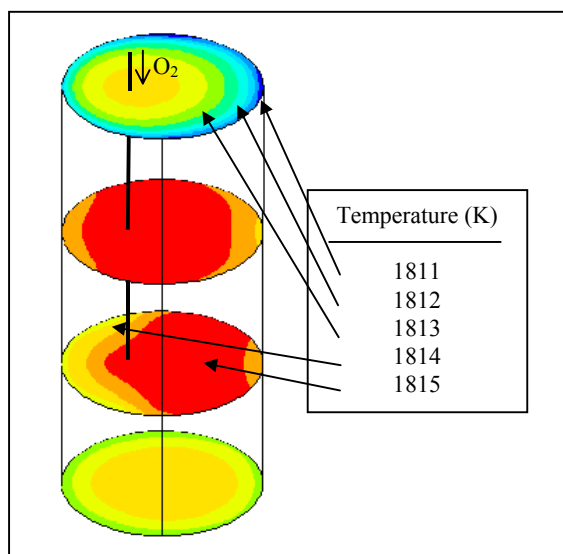


**Figure 7:** Temperature distribution during desulfurization process.

The concentration fields of dissolved (CaS) and (CaO) as well as that of  $\{O_2\}$  and  $\{SO_2\}$  bubbles are given in Figure 5. In this simulation a homogeneous (CaS) concentration of 1 % is assumed at the beginning. The amount of oxygen injection is set constant during the process. A significant disadvantage of these properties is that the spacial concentration distributions are hardly measurable in hot temperature experiments.

The temperature distribution in several horizontal planes is given in Figure 7. Heat is produced by the exothermic desulfurization reaction at the submerged lance tip while it is lost at the bath surface and at walls. The hottest spot at the bath surface indicates the stagnation point of the uprising hot plume. As the surface temperature distribution is measurable in hot temperature experiments this simulation result can be validated.

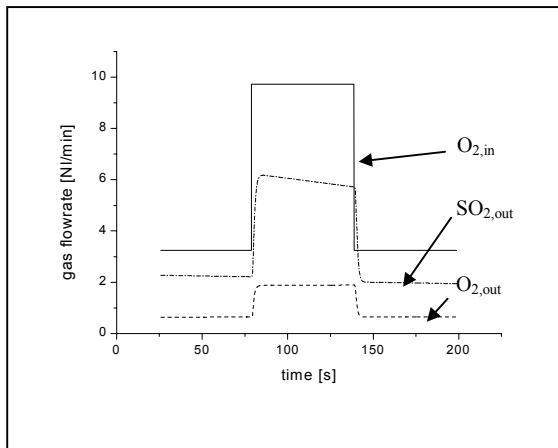


**Figure 8:** Offgas composition during stepwise oxygen injection

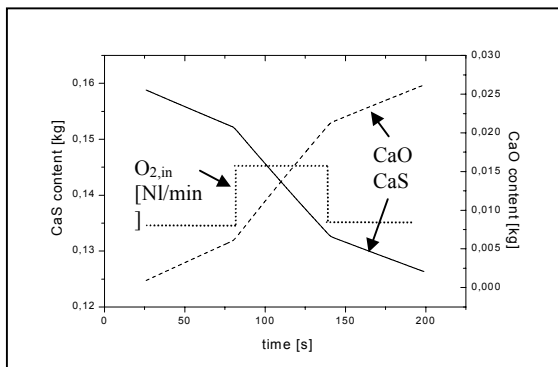


**Figure 9:** (CaS) decrease and (CaO) accumulation during stepwise oxygen injection.

In order to study the time dependent variation of the offgas composition the lance is supplied by stepwise varied oxygen throughput. Figure 8 shows the  $\{O_2\}$  and  $\{SO_2\}$  content of the offgas during this simulation. The solid line indicates the oxygen flow rate variation. It should be possible to measure the offgas composition online in real experiments.

The same simulation is performed to examine the time-dependent desulfurization rate of the slag. Figure 9 depicts the variation of the (CaS) and (CaO) content in the slag. Due to the desulfurization reaction calcium exchanges a

sulfur atom with an oxygen atom. Therefore the two curves differ from each other only by a negative sign. The composition of the slag can be measured only at a couple of distinct time steps. Therefore comparison with these simulation results is rather limited.

## CONCLUSION

A simulation tool for the calculation of a new desulfurization process is presented. This technology can be divided into two main steps, which can be treated separately. During the development of the simulation tools special care is taken to generate simulation results that can be compared with high temperature results. The main conclusions of this study are

- The coupled simulation of the hot metal desulfurization process including chemical interface reactions and thermal considerations in hot metal and slag phases, turns out to be feasible. Parameter variations prove that the implemented models work reasonably.
- As hot metal desulfurization is controlled by transport mechanisms the flow pattern in the liquid phases determines the reaction rate. Therefore porous plug position as well as gas flow rate influences the desulfurization rate as can be shown with the help of CFD.
- The simulation of the slag regeneration process also seems to be feasible and parameter studies work well.
- CFD turns out to be a powerful investigation tool for metallurgists as soon as in the design phase of new technologies.

## REFERENCES

- DEO B. and BOOM R. (1993), "Fundamentals of Steelmaking Metallurgy", *Pretice Hall International*, New York, USA.
- FLUENT INC. (1996), "FLUENT User's Guide - Release 4.4", *Fluent Incorporated*, Lebanon, USA.
- GLOVATSKII V.A. et al. (1982), "Regeneration of blast furnace slags used for desulphurizing pig iron", *Steel in the USSR*, pp. 246-248.
- LAUNDER B.E. and SPALDING D.B., (1972), "Lectures in Mathematical Models of Turbulence", *Academic Press*, London, England.
- MANNINEN M.; TAIVASSALO V. and KALLIO S. (1996), "On the mixture model for multiphase flows", *VTT Publications 288*, Espoo, Finland.
- OETERS F. (1989), "Metallurgie der Stahlherstellung", *Verlag Stahleisen*, Düsseldorf, Germany.
- PATANKAR S.V. (1980), "Numerical Heat transfer and Fluid Flow", *Hemisphere Publishing Corporation*, New York, USA.
- PRANDTL L.; OSWATITSCH K. and WIEGHARDT K. (9. Edition, 1993), "Führer durch die Strömungslehre", *Vieweg*, Braunschweig, Germany.
- RAY H.S. (1993), "Kinetics of Metallurgical Reactions", *Science Publishers, Inc.*, Lebanon, USA.